# Advanced optical modeling of thin metals for improved robustness and accuracy of scatterometric models

Carsten Hartig[1], Adam M. Urbanowicz[2], Dmitriy Likhachev[1], Ines Altendorf[1], Andreas Reichel[1], Martin Weisheit[1]

[1]GLOBALFOUNRIES, Dresden, Germany
[2]NOVA EU, Dresden, Germany

*Abstract* — **The majority of scatterometric models used in production control assume constant optical properties of the materials included into the film stack. Only dimensional parameters are assumed as the degrees of freedom. This assumption negatively impacts model precision and accuracy (especially with the trend of scaling down the critical dimensions). In this work we focus on the modeling of Cu and TaN/Ta optical properties in back-end-of-line applications and consider the impact of Cu optical properties modifications in the trenches and as a substrate. We also consider the Cu transparency threshold when Cu acts as a substrate in the film stack. In the case of ultrathin Cu substrate the model output becomes invalid. Quite frequently this fact is not reflected in the goodness of fit. We show that accurate optical modeling of Cu is essential to achieve the required scatterometric model quality for automatic process control in microelectronic production. As a result, we obtain appreciably better matching with electrical data. Therefore, electrical performance can be predicted early in production flow. The modeling methodology presented here can be applied for all technology nodes and also other thin metals such as Co and Ru.**

***Keywords* — *Cu, Cu transparency threshold, optical properties, thin metals, optical modeling, scatterometry, OCD***

## I. Introduction

At present time, the accuracy requirements for optical critical dimension (OCD) metrology (a.k.a. "scatterometry") grow gradually with new technology nodes and high-yield demand. Most of the OCD models assume constant optical properties of the materials. Typically, the model selection rules are based on a given design-of-experiment (DoE) wafer optimization, specific hardware sensitivity, and desired parameter of interests [1]. However, with growing requirements regarding automatic process control, wafer zone control, and shrinking dimensions, the typical assumptions become insufficient. Discrete modeling problems start to reveal themselves. Here we demonstrate one of such examples in back-end-of-line (BEOL) applications based on large data statistics. The assumption of constant optical properties starts to affect accuracy of the OCD model. Furthermore, understanding the causes of optical properties variation of given material can result in new model parameters that can be utilized for process control. Example discussed in this paper is ultra-thin Cu in trenches. The Cu resistance grows rapidly with thicknesses comparable to the electron mean free path length in Cu (around 40 nm). The resistance change is also reflected in optical properties of the material. This fact can be utilized for improved process control. On the other hand, scaling down dimensions causes new challenges for optical modeling. The ultra-thin metal layers have optical properties dependent on thickness. This in turn affect OCD model performance. Therefore, variation of thin metals optical properties needs to be explored and properly assumed in the modeling. We discuss the effect of free and bounded electrons for the thickness regime close to the electron mean free path length using Cu metal as an example. This can enable easier optical model construction for various thin metals used in microelectronics (such as Co, Ru, W, etc.). The effect of optical properties variation on scatterometric model performance needs to be studied case by case due to various relative material volume, specific correlation and optical properties changes for a given material. In this work we focus on BEOL polish OCD application.

## II. Results and Discussion

We split discussion into three sections. First, we discuss general problems related to modeling of thin metals. Then we present the modeling result for Cu and TaN metals. And, finally, we apply the advanced metal models in scatterometric modeling.

### A. *Main factors influencing optical properties of thin metals*

Modeling of the thin metal properties is a real challenge in optical analysis due to thickness dependence of the optical properties. The optical properties of thin-metal films vary with deposition conditions, surface oxidation/roughness and film thicknesses [2-4]. We propose a new classification of the regimes of optical properties of polycrystalline metals for OCD modeling needs: (1) below percolation threshold when the metal forms islands and shows metal-insulator transition [5]; the other regime is (2) when the metal thickness level becomes comparable with its electron free path; and finally (3) the bulk regime where the thickness is much greater than the electron free path. The latter two regimes are relevant for OCD modeling. It is a known

technology challenge that Cu resistivity increases with shrinking diameter of the wire (100 nm and below). This occurs when wire dimensions are in the range of the mean free path of electrons (about 40 nm for Cu at room temperature). This is also the reason for new BEOL integration approaches based on Ru and Co metals [6]. It is, however, less known that shrinking dimensions of wires also cause metrology challenges due to optical properties variations of metals. There is a clear connection between metal electrical resistivity and its optical properties. The resistivity of narrow trenches is defined by surface scattering (Fuchs-Sondheimer (FS) model [7]) and grain boundary scattering (Mayadas and Shatzkes (MS) model [8]). Grain boundary scattering assumes Cu grain boundary reflectivity and it is shown to be the main contributor to thin Cu resistivity [9]. The MS approach was extended by Sotelo et al. to study optical properties of polycrystalline metal thick films in the visible and far infrared range of the spectrum [10]. It was demonstrated that grain boundary scattering is responsible for lowering of the metal film reflectivity with its grain size. Finally, Yakubovsky et al. showed a link between structural morphology and optical response for the thickness range of 20-200 nm that corresponds to the typical Cu wires sizes [11]. A strong dependence on grain scattering was found for Au below 66 nm of thickness (findings applicable for Cu, Ag metals). The optical properties of metals can be approximated as additive contributions of bounded electrons described by the Lorentz model and free electrons described by the Drude model. For thin metals in the thickness regime comparable to the mean free path length of the electrons, the free-electron contribution is affected more strongly by microstructural changes than the bounded-electron contribution. The free-electron contribution described by the Drude model is expressed as follows (eq. 1):

$$\varepsilon = \varepsilon' + i\varepsilon'' = \varepsilon_\infty - \frac{\omega_p^2}{\omega^2 + i\gamma\omega} = \varepsilon_\infty - \frac{\omega_p^2}{\omega^2 + \gamma^2} + i\frac{\gamma\omega_p^2}{\omega(\omega^2 + \gamma^2)} \quad (1)$$

Here, $\varepsilon_\infty$ is the dielectric constant at infinite frequency, $\omega_p$ is the plasma frequency, and $\gamma$ is the damping constant. $\gamma$ is equal to the electron relaxation rate in a polycrystalline metal and can be represented by a sum of $\gamma_{ep}$ – electron-phonon scattering, $\gamma_{eg} = \gamma_{eg}(D)$ – electron grain boundary scattering rate, and $\gamma_{es} = \gamma_{es}(t)$ – scattering from the film surface. According to this model, metal structure dependent contributions $\gamma_{eg}(D)$ and $\gamma_{es}(t)$ become larger with decreasing of average grain size D and film thickness t. The optical dependence on thickness was observed in the range of 5 nm to 40 nm of Cu [12]. The Cu grain size distribution and orientation in trenches was studied in literature: the desired Cu microstructure has maximum crystal size and bamboo-like grain structure [13]. Both electrical resistance and optical properties are influenced by the grain size in trenches. The Cu grain size and resistance are dependent on many process factors such barrier conditions, electrodeposition conditions, temperature, and trench dimensions [14]. Besides Cu, other metals are present in the trenches. The typical barrier contains TaN and Ta [15].

*B. Modeling of thin Cu and TaN metals*

*a) TaN modeling.* Thin TaN films were deposited on Si wafers with 400 nm oxide. The target thickesses were in the range from 20 to 80 Angstroms. Figure 1 shows the optical properties of the production grade TaN films with various thicknesses. The optical properties exhibit strong thickness dependence and metallic behavior down to the smallest thickness. TaN itself can have up to five different phases, ranging from resistive to conductive, and each phase reflects different optical properties [15].

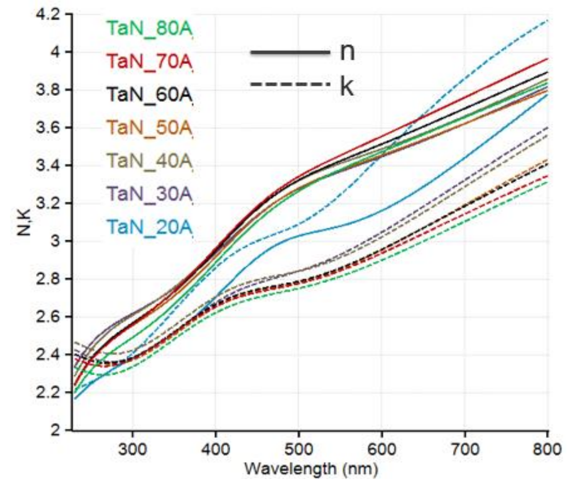

Figure 1. Thickness dependence of production grade TaN on optical properties.

The TaN thickness is closer to 20 Å in real production flow. It also can be seen that the 20 Å curve deviates (light blue) from the set. Furthermore, TaN optical properties vary with thickness and deposition conditions. However, the barrier materials have secondary effect on the OCD model since the effective material volume is smaller than that of Cu. The effects due to variability of dielectric materials on accuracy of scatterometric measurements have been discussed by the authors earlier [16,17].

*b) Cu modeling – thin Cu effect:* We used 300 mm Si wafers with 400 nm of $SiO_2$ as an interference enhancement layer, Ta and Cu layers. Cu was deposited using a Cu seed and electroplating process as in the standard production flow. The prepared wafers were thinned by CMP (chemical-mechanical polishing), with thickness targets of 400, 600, 800, 1000, 1500, and 2000 Angstroms. These unpatterned test wafers were measured using XRR, resistance and optical thickness metrology. The film stack resistivity as a function of XRR measured thicknesses is shown in Figure 2. The polishing process was non-uniform across the wafers resulting in additional Cu thickness variation. It should be mentioned that the resistvity measurements were performed on whole Ta/Cu system. The reading is close to the bulk Cu resistivity for the case of a continuos Cu layer. There could be some small error for reistivity values, however the general resistivity trend is correct and agrees with literature data.

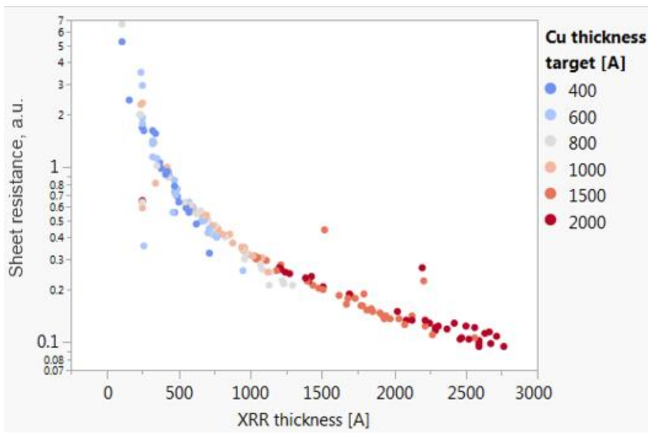


Figure 2 Sheet resistance (log scale) vs thickness measured (linear scale) by XRR for unpatterned wafers polished with different thickness targets.

The Cu film becomes transparent in some wavelength ranges with a threshold around 800– 850 Å (see also Figure 11). Figure 3 shows measured reflectivity data for the Cu films with thicknesses below and above transparency threshold. When Cu becomes transparent, the interference fringes from the $SiO_2$ layer underneath become visible.

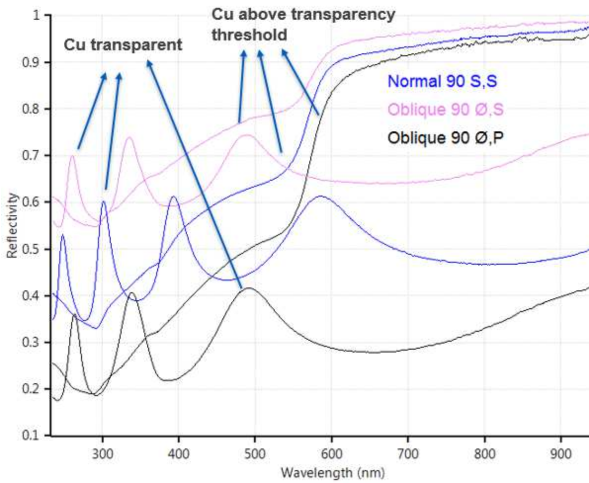


Figure 3. Reflectivity spectra for Cu with thicknesses below (interference fringes are visible) and above transparency threshold (around 800 Å).

In a first modeling approach, reflectometry measurements of Cu layers with thicknesses ranging from very thin and transparent (10nm) to thick and fully opaque (200nm) were used to extract the parameters for a sum of one Drude and 4 Tauc-Lorentz (TL) oscillators. The parameters of the TL oscillators (the range below 600nm in Fig. 4), which correspond to the bound-electron states, were found to be changing very weakly with Cu thickness and were subsequently fixed at their average values. The amplitude of the Drude oscillator, on the other hand, shows significant response to the Cu thickness. The oscillator width / damping constant was less sensitive and fixed at 0.03eV to make the model more robust. Fig. 4 shows the (n, k) curves for several Drude amplitudes in the completed model, where the lowest correspond to extremely thin Cu of 7μΩcm. Using this model, we were able to reliably fit the thickness of a Cu film with strong variations across the wafer (Fig. 4b).

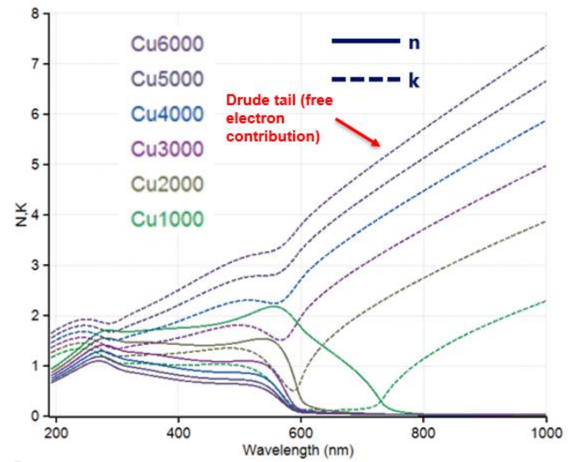


Figure 4 (n,k) spectra of the fully parameterized model, which assumes Drude amplitude only as floating parameter.

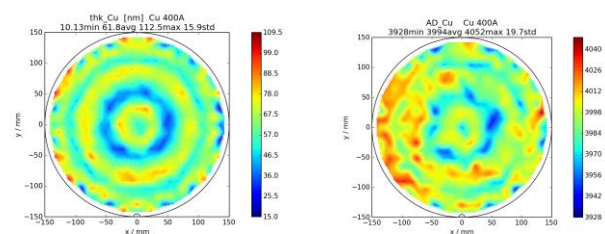


Fig. 4b: Thickness (left) and Drude amplitude (right) of an unpatterned Cu film with strong thickness variations

In addition, we used a conventional multi-oscillator approach to extract the Cu optical properties at various Cu thicknesses from our set that are more relevant for production. The optical properties are shown in Figure 5. The variations in Drude contribution ($k$ values close to 1000 nm) shows increased Drude resistivity compare to bulk Cu. However, current $k$ trend with film thickness in near-infrared region is not that clear.

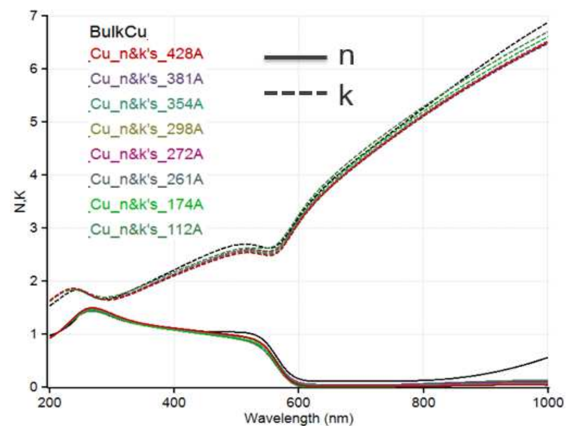


Figure 5 Optical properties extracted from Cu DoE data by using conventional multi-oscillator fit.

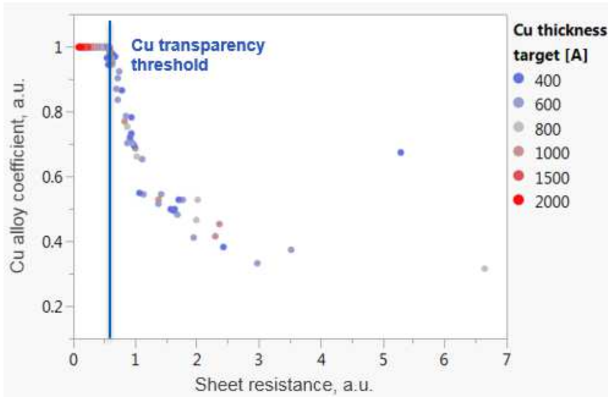

Figure 6 Alloy coefficient vs sheet resistance changes.

To build the Cu model that would be used as an input for scatterometry modeling we use an alloy model concept. The alloy coefficient acts an interpolant between modeled (*n,k*)-curves for different Cu thicknesses. The alloy coefficient range is from 0 to 1. In our case unity corresponds to bulk material while the values close to zero correspond to the *n&k*'s of thin Cu films. One of the important questions is how the alloy coefficient responds to the changes in resistivity of Cu. This relation is illustrated Figure 6. Obviously, when the Cu thickness starts to approach a value of 800 Å, we would get the bulk Cu optical properties and the alloy coefficient value of 1. For the lower Cu thicknesses, we observe that the alloy coefficient correlates with Cu resistivity. Another question would be to compare the model's outputs with XRR thickness and Cu resistivity data. This relation is presented in Figure 7. XRR can measure Cu thickness for whole thickness range while reflectometry only can do that for the thicknesses below the transparency threshold. Therefore, we can only compare the thickness values for the case of partially transparent Cu. We observe the same trend as for XRR but with some offset. Also, we converted the alloy coefficient behavior into corresponding Cu thicknesses (we call it a "fictitious thickness"). The result is displayed in Figure 7 by a red curve.

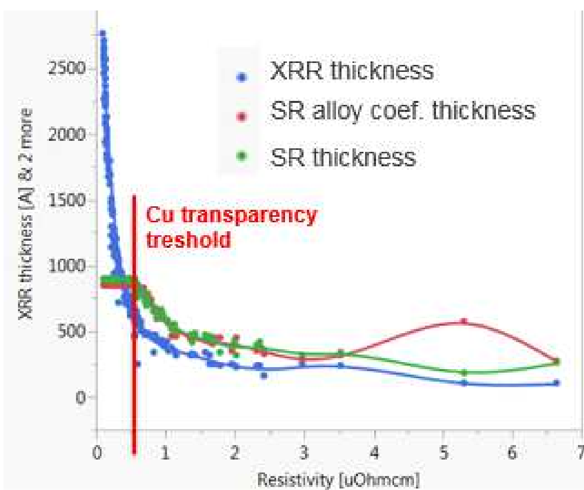

Figure 7 The thickness values measured by XRR (blue line), SR (green line), and the SR fictitious thicknesses, estimated based on the alloy coefficient as functions of Cu resistivity.

Despite basic performance we focus which Cu optical properties changes the most. We compared Cu optical properties shown in figures 4,5 and 7. We can see that more changes in WL above 600 nm occur for more for set with varied thicknesses of Cu (figures 4 and 5) than for figure 8 where we present model variation that describe bulk Cu variation (as substrate). This can support the theoretical considerations in chapter A that for thin Cu there is more impact from free electrons.

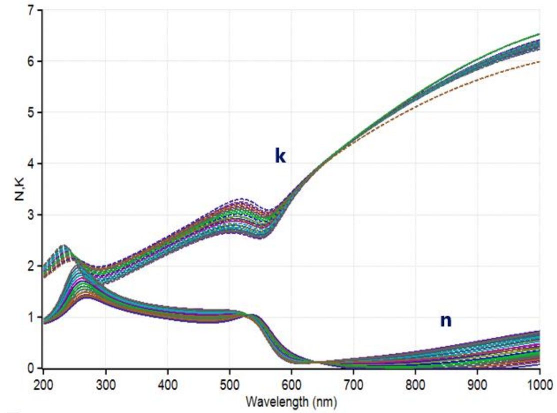

Figure 8 The variation of optical properties of bulk-Cu used as a substrate for broad range of production data. The nk curves are generated by using floating parameters of the multi-oscillator production model in the valid range.

*C. Application of an advaned thin metal model in a scatterometry solution*

Usually, the Cu wire resistance data (Kelvin probe) correlate with trench height (also trench volume). Typical M2 trench structure is shown in Figure 9. As can be noted that the larger the trench height and, therefore, the Cu wire cross-section, the smaller the resistance (as shown in Figure 10). Moreover, as one can also see, the correlation between the electrical data and optically measured Cu trench height is noticeably worse for the points with wafer's radius larger than 12 cm.

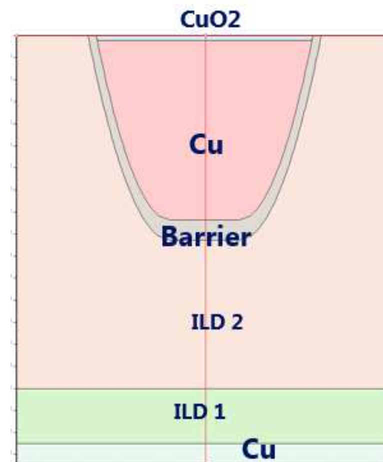

Figure 9. Typical M2 Cu trench structure.

The development of a mature product typically includes yield optimization at wafer edge. However, in practice a wafer edge reveals many process problems and often the material properties of the layers as well as Cu substrate can vary from wafer's center to edge. Therefore, the assumption

of constant optical properties for the Cu and/or barrier layer may significantly affect the accuracy of scatterometry measurements. For improved accuracy the Cu optical properties can be floated. Typical variations of the Cu (effective model substrate) material properties are shown in Figure 8. These results were obtained from real production data by floating the Cu dispersion model. The main challenge related to the Cu substrate is the critical thickness when Cu becomes transparent and is no longer can be treated as a bulk substrate. In that case, the light can penetrate through the Cu layer and this fact leads to a necessity to include the underlying layers into the model. As shown in Figure 11, around 1% of incoming light with some wavelengths will penetrate through the Cu layer with thickness of 70 nm. The Cu transparency threshold is marked by dashed red line in Figure 11 (around 800 Å). It is unclear how much of the signal from layers below Cu substrate is enough to have significant effect on reflectance spectra (we can roughly estimate around 1% or five penetration depths of light passing through Cu substrate have effect on optical model output). However, the important observation is that spectral area from 500 nm to 600 nm is characterized by higher light penetration through Cu. This area is also the spectral range of significant reflectance change due to Cu and dielectric heights in OCD model. The light penetration through the Cu substrate results in incorrect OCD model output. Also, in some cases, possible correlations between the fit parameters can lead to their multiple combinations which could result in numerous acceptable values of the merit function as an alternative to the true global minimum. Additionally, the Cu transparency is wavelength dependent and often the range between 500 and 600 nm is highly responsible for the height and dielectric sensitivities. Therefore, it is necessary to develop additional metrics that indicate a problem due to thin Cu substrate. One of the directions is accurate modeling of Cu. The Cu substrate can have a certain grain size gradient that changes with thickness. Additionally, the Cu in trench also changes its optical properties due to dimensional constraints. For instance, Cu CD value of approximately 40 nm is comparable with the electron mean free path length in Cu. To overcome those challenges, we developed improved dispersion models for the Ta/TaN barrier, bulk Cu and Cu in trenches. We have compared how the OCD model output correlates with electrical data. Figure 10 represents the electrical data correlation to the Cu trench height and figure 12 compare the Cu material parameter (alloy coefficient) with electrical data. Both figures based on large data set of almost 800 wafers. Each point constitutes a wafer's average quantity under measure for two wafer's areas with radii less (red dots) and more (blue dots) than 12 nm. Such data averaging and zone splitting were necessary due to distance spacing between OCD test pads and electric test structures. We found that the alloy coefficient of the Cu model in the trench correlates better than the commonly used trench height/volume parameters (see Fig. 10 and Fig. 12). Moreover, the split between central and edge areas of wafer was significantly reduced as shown in Figure 12. In summary, we believe that the optimal solution is to use both dimensional and material parameters to improve the correlation of the scatterometric model with electrical data.

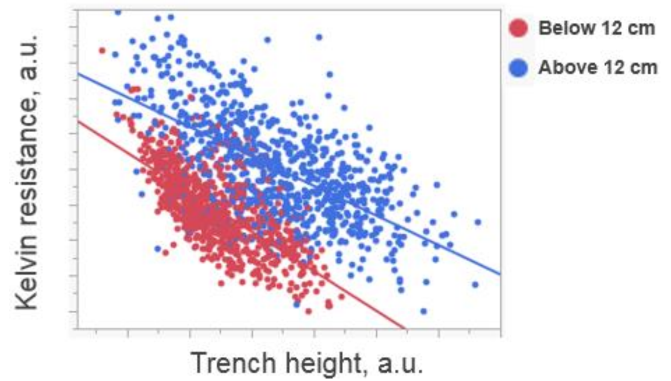

Figure 10. Correlation of the Cu trench height with Kelvin resistance. Red data represent average values for 0 to 12 cm radius of a 300 mm of wafer and blue data above 12 cm wafer radius.

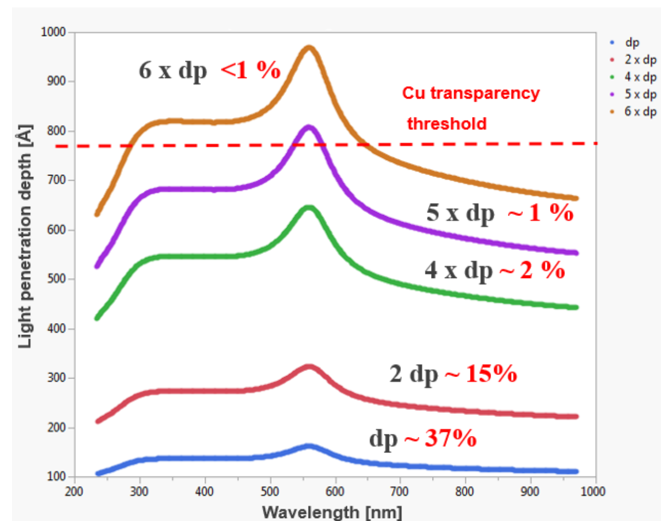

Figure 11 Depth of penetration calculated using the Cu extinction coefficient. Red-colored values indicate the light intensity at correspondent depths (in percentage of its initial/surface value). The dashed line marks Cu transparency threshold.

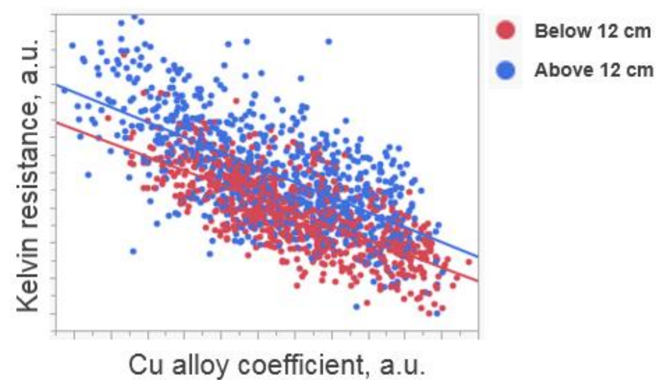

Figure 12. Correlation of the Cu alloy coefficient height with Kelvin resistance. Red data represent average values for 0 to 12 cm radius of a 300 mm of wafer and blue data above 12 cm wafer radius

## III. CONCLUSIONS

We discused the main factors influencing the optical properties of ultra-thin metals. We demonstrate that the optical properties of thin TaN barrier layer are strongly thickness dependent. We explored the Cu optical properties when Cu thickness is  comparable with its electron free path length of around 40 nm. This variaiton of optical propeties is mainly due to the free electron contribution to the dielectric function. Finally, we show that these enhanced metal models can improve scatterometric model performance in terms of electrical data correlation. We propose to use a floating material parameter for Cu in trench as an additional parameter to improve correlation to electrical data. This study demonstrated that ultra-thin Cu/TaN metals films show significant variation of optical properties. The similar modeling approach can be applied for other ultra-thin metals utilized in mircroelectronics such as Co, Ru, or W. The electron free mean path length is known for each metal and can indicate the thickness regime of significant change of optical properties due to free electron contribution. The future work should focus on more accurate descripton of optical properties of various ultra-thin metals utilized in microelectronics. The correctly described optical properties variation enables an increased accuracy and faster time to solution of OCD applications. Furhtermore, the approach enable correct modeling of accuracy and precission impact due to metal optical properties variation for future technology nodes. Typically, dimensional variation is specified and depends on specific process steps in the OCD model where optical properties are assumed constant. This simplification becomes invalid in the cases of significant within-wafervariation of optical properties of the material layers, especially metals that are characterized by strong optical contrast.

## REFERENCES


[1] G. K. P H. Fujiwara, Ed., Spectroscopic Ellipsometry: Principles and Applications, John Wiley & Sons Ltd, (2007)

[2] G. K. Pribil, B. Johs, and N. J. Ianno, "Dielectric function of thin metal films by combined in situ transmission ellipsometry and intensity measurements," Thin Solid Films 455–456(0), 443-449 (2004).

[3] C. Liu et al., "Thickness determination of metal thin films with spectroscopic ellipsometry for x-ray mirror and multilayer applications," Journal of Vacuum Science & Technology A: Vacuum, Surfaces, and Films 17(5), 2741-2748 (1999).

[4] M. Hövel, B. Gompf, and M. Dressel, "Dielectric properties of ultrathin metal films around the percolation threshold," Physical Review B 81(3), 035402 (2010).

[5] T. Nogami, X. Zhang, J. Kelly et al., "Comparison of key fine-line BEOL metallization schemes for beyond 7 nm node." T148-T149.

[6] E. H. Sondheimer, "The mean free path of electrons in metals," Advances in Physics, 1(1), 1-42 (1952).

[7] A. F. Mayadas, and M. Shatzkes, "Electrical-Resistivity Model for Polycrystalline Films: the Case of Arbitrary Reflection at External Surfaces," Physical Review B, 1(4), 1382-1389 (1970).

[8] W. Steinhögl, G. Schindler, G. Steinlesberger et al., "Size-dependent resistivity of metallic wires in the mesoscopic range," Physical Review B, 66(7), 075414 (2002).

[9] J. Sotelo, J. Ederth, and G. Niklasson, "Optical properties of polycrystalline metallic films," Physical Review B, 67(19), 195106 (2003).

[10] D. I. Yakubovsky, D. Y. Fedyanin, A. V. Arsenin et al., "Optical constant of thin gold films: Structural morphology determined optical response," AIP Conference Proceedings, 1874(1), 040057 (2017).

[11] Gong, Jun-Bo, Wei-Le Dong, Ru-Cheng Dai, Zhong-Ping Wang, Zeng-Ming Zhang, and Ze-Jun Ding. "Thickness Dependence of the Optical Constants of Oxidized Copper Thin Films Based on Ellipsometry and Transmittance." Chinese Physics B 23, no. 8 (2014): 087802.

[12] S. Maitrejean, V. Carreau, O. Thomas et al., "Cu Grain Growth in Damascene Narrow Trenches," AIP Conference Proceedings, 1143(1), 135-150 (2009).

[13] C. Yang, T. Standaert, H. Huang et al., "Line Resistance Reduction in Advanced Copper Interconnects," IEEE Electron Device Letters, 38(11), 1579-1582 (2017).

[14] L. Gerlich, S. Ohsiek, C. Klein et al., "Interface engineering for the TaN/Ta barrier film deposition process to control Ta-crystal growth," Microelectronic Engineering, 106(0), 63-68 (2013).

[15] C. Stampfl, and A. J. Freeman, "Stable and metastable structures of the multiphase tantalum nitride system," Physical Review B, 71(2), 024111 (2005).

[16] A. M. Urbanowicz, P. Ebersbach, D. Likhachev et al., "In-line control of material properties of SiOC:H based low-k dielectrics utilizing optical metrology AM: Advanced metrology." 24-28 (2017).

[17] C. Hartig, A. M. Urbanowicz, A. Vaid et al., "Practical aspects of TMU based analysis for scatterometry model referencing AM: Advanced metrology." 34-39 (2017).Trans. Roy. Soc. London, vol. A247, pp. 529–551, April 1955. *(references)*